AGU PUBLICATIONS

Geophysical Research Letters

RESEARCH LETTER
10.1002/2016GL072071

Key Points:
- Deep troughs (700 m) beneath major ice shelves in the Amundsen Sea sector of Antarctica reveal pathways for warm waters to melt glaciers
- Bed mapping extends in a seamless fashion from multibeam offshore to high-resolution reconstruction inland for the first time
- The data should be an important asset for ice sheet and ocean modelers and improve our understanding of this sector

Supporting Information:
- Supporting Information S1

Correspondence to:
R. Millan,
millanr1@uci.edu

Citation:
Millan, R., E. Rignot, V. Bernier, M. Morlighem, and P. Dutrieux (2017), Bathymetry of the Amundsen Sea Embayment sector of West Antarctica from Operation IceBridge gravity and other data, *Geophys. Res. Lett.*, *44*, 1360–1368, doi:10.1002/2016GL072071.

Received 23 NOV 2016
Accepted 5 JAN 2017
Accepted article online 9 JAN 2017
Published online 4 FEB 2017

Bathymetry of the Amundsen Sea Embayment sector of West Antarctica from Operation IceBridge gravity and other data

Romain Millan[1], Eric Rignot[1,2], Vincent Bernier[1], Mathieu Morlighem[1], and Pierre Dutrieux[3]

[1]Department of Earth System Science, University of California, Irvine, California, USA, [2]Jet Propulsion Laboratory, Caltech, Pasadena, California, USA, [3]Lamont-Doherty Earth Observatory, Columbia University, Palisades, New York, USA

Abstract We employ airborne gravity data from NASA's Operation IceBridge collected in 2009–2014 to infer the bathymetry of sub–ice shelf cavities in front of Pine Island, Thwaites, Smith, and Kohler glaciers, West Antarctica. We use a three-dimensional inversion constrained by multibeam echo sounding data offshore and bed topography from a mass conservation reconstruction on land. The seamless bed elevation data refine details of the Pine Island sub–ice shelf cavity, a slightly thinner cavity beneath Thwaites, and previously unknown deep (>1200 m) channels beneath the Crosson and Dotson ice shelves that shallow (500 m and 750 m, respectively) near the ice shelf fronts. These sub–ice shelf channels define the natural pathways for warm, circumpolar deep water to reach the glacier grounding lines, melt the ice shelves from below, and constrain the pattern of past and future glacial retreat.

1. Introduction

The Amundsen Sea Embayment (ASE) in West Antarctica (West Antarctic Ice Sheet (WAIS)) is a major contributor to present-day sea level rise from Antarctica and holds an ice volume equivalent to 1.2 m global sea level rise [e.g., *Rignot*, 2008]. The major glaciers in the ASE include the Pine Island, Thwaites, Haynes, Smith, Pope, and Kohler glaciers. These glaciers are retreating along deep troughs with a bed elevation that decreases inland, a factor long recognized to promote rapid, irreversible retreat [e.g., *Hughes*, 1981]. Several studies have suggested that this sector of WAIS may already be in a state of collapse [*Parizek et al.*, 2013; *Favier et al.*, 2014; *Joughin et al.*, 2014; *Rignot et al.*, 2014]. A number of airborne radar surveys were conducted to measure ice thickness and bed topography on land [*Thomas et al.*, 2004; *Holt et al.*, 2006; *Vaughan et al.*, 2006; *Leuschen et al.*, 2010]. *Fretwell et al.* [2013] combined these data with year 2008 GEBCO bathymetry data to produce the bed topography BEDMAP-2 which includes the sea floor depth. A considerable amount of bathymetric data, including multibeam echo sounding (MBES) data, was subsequently assembled as part of International Bathymetric Chart of the Southern Ocean (IBCSO) [*Arndt et al.*, 2013; *Nitsche et al.*, 2007], but data coverage did not extend into the sub–ice shelf cavities. As a result, bed mapping between the glacier grounding lines and the ice shelf fronts has been affected by large uncertainties. For example, the BEDMAP-2 and IBCSO bathymetries beneath Crosson and Dotson ice shelves assume zero water column; i.e., the sea floor depth coincides with the ice shelf draft. Such gap in our knowledge makes it difficult to study ice-ocean interactions beneath these ice shelves. Data from neighboring regions [e.g., *Jenkins et al.*, 2010] show that deep channels carved on the seafloor by past advances of the glaciers exist beneath all these ice shelves. These bed troughs act as natural pathways for subsurface, warm, salty, Circumpolar Deep Water (CDW) to reach the glacier grounding lines [*Jacobs et al.*, 2011]. Warm CDW induces high rates of ice shelf melt [*Rignot et al.*, 2013] that exert an important control on glacier flow and stability. Conversely, sills in the seafloor or stranded icebergs may partially block the access of CDW to the glaciers [*Jacobs et al.*, 2012]. Resolving the bathymetry beneath the ice shelves is, therefore, a fundamental prerequisite to investigations of ocean circulation near the coastline, its impact on ice-ocean interactions and glacier retreat, and in turn on understanding the past, present, and future mass balance of this sector of WAIS.

On land, the results of airborne radar surveys have been combined with high-resolution ice flow vectors from satellite radar interferometry using a mass conservation method (MC) [*Morlighem et al.*, 2011] to produce the first high-resolution (350 m), gridded map of ice thickness and bed topography upstream of the grounding

lines of all ASE glaciers [*Rignot et al.*, 2014]. These products have revealed erroneous bed picking from the radar echoes beneath Pine Island caused by bottom crevasse formation during the rapid glacier retreat that took place in the years of 2004–2009. Fresh bottom crevasses yield strong radar echoes at their apex that are confused with echoes from the ice shelf draft. The corrected data revealed a deeper bed at the grounding line and the absence of major sills in topography upstream that could halt the glacier retreat. Similar conclusions of unstoppable retreat were reached for Thwaites, Haynes, Pope, Smith, and Kohler glaciers, but the shape of the sub–ice shelf cavities in front of these glaciers remains poorly sampled. This is important to resolve because the shape of the cavities determines how ocean heat reaches the glacier grounding lines, which in turn determines whether the retreat will be rapid (warm water access, high melt) versus slow (no warm water access, low melt).

Since 2009, NASA Operation IceBridge (OIB) has been collecting airborne gravity data to constrain the bathymetry beneath these ice shelves [*Cochran and Bell*, 2010]. These data have been complemented by in situ measurements beneath Pine Island Shelf from an Autonomous Underwater Vehicle (AUV) [*Jenkins et al.*, 2010] and from seismic methods [*Muto et al.*, 2016, M2016]. On Pine Island, both data sets revealed the presence of an east-west ridge across the ice shelf path that probably acted as an anchor in the past [*Jenkins et al.*, 2010; *Studinger et al.*, 2010] and modulates the access of CDW to the grounding line [*Dutrieux et al.*, 2014]. On Thwaites, *Tinto and Bell* [2011] applied two-dimensional (2-D) inversions on data from year 2009 to reveal a prominent ridge, 15 km wide, with two peaks, 40 km from the present front, that may have pinned down the glacier in the past. No result has been published for Crosson and Dotson ice shelves farther west. More importantly, none of the gravity data have been analyzed and inverted in a seamless fashion to provide consistent topography across the grounding line, match the MBES/IBCSO data offshore, and the MC bed topography inland. This lack of consistency across the grounding zone significantly affects data quality and limits what can be done with ice sheet and ocean numerical models using these data. In particular, large discontinuities in bed topography across the grounding line are a major impediment to correctly reconstruct ice flow evolution.

Here we employ a methodology that combines the OIB gravity data from years 2009 to 2014 with high-resolution MC bed mapping inland and MBES/IBCSO mapping offshore using a three-dimensional (3-D) inversion to obtain a consistent and comprehensive bed topography across the entire ASE domain beneath ice shelves and extending along the glacier grounding lines. In addition, for Pine Island, we use the AUV and seismic data collected on the shelf to constrain the inversion. We estimate the uncertainty of the inversion and discuss the impact of the results on the identification of natural pathways of CDW toward the grounding lines, their impact on the ice shelf melt regimes, and their impact on the past, present, and future pattern of glacial retreat.

2. Data and Methods

We use OIB gravity measurements acquired between October 2009 and November 2014 by the Sanders Geophysics Airborne Inertially Referenced Gravimeter (AIRGrav). AIRGrav flies a draped survey at about 400 m above ground on average [*Cochran and Bell*, 2010]. The gravimeter measures the Earth's gravity field and accelerations at a sampling frequency of 128 Hz. Anomalies are decimated to 2 Hz. Data are filtered and delivered at a spatial resolution of 4.9 km in this area using a 70 s full wavelength filter at an aircraft speed of 150 m/s. Eotvos, normal gravity, free-air, static, and level corrections are applied on the data to yield free-air gravity anomalies, which we refer to as gravity data in the remainder of the paper. An analysis of crossovers indicates a measurement error of 0.5 mGal for the gravity data.

We select 32 OIB tracks with an absolute elevation of less than 1500 m above mean sea level (Figure S1 in the supporting information). All data are upward continued to the maximum plane elevation within the survey domain; i.e., the gravity data collected at various elevations are extrapolated upward to a common elevation which is the highest aircraft elevation within the survey. We divide the survey domain into three blocks for ease of computation: (1) Pine Island, (2) Thwaites, and (3) Kohler and Smith glaciers, with Haynes split between domains 2 and 3 (Figure 1). The gravity data are "upward continued" to 1600 m for Pine Island, 1700 m for Thwaites, and 2000 m for Kohler/Smith. We employ the Geosoft GM-SYS 3-D software which implements *Parker*, 's [1973] method on a 3-D representation of the study area with three horizontal layers: (1) a solid ice layer with a density of 0.917 g/cm^3; (2) a seawater layer with a density of 1.028 g/cm^3; and (3) a rock/sediment substrate layer with a uniform density of 2.88 g/cm^3. Density selection for rock is discussed later on. Ice surface

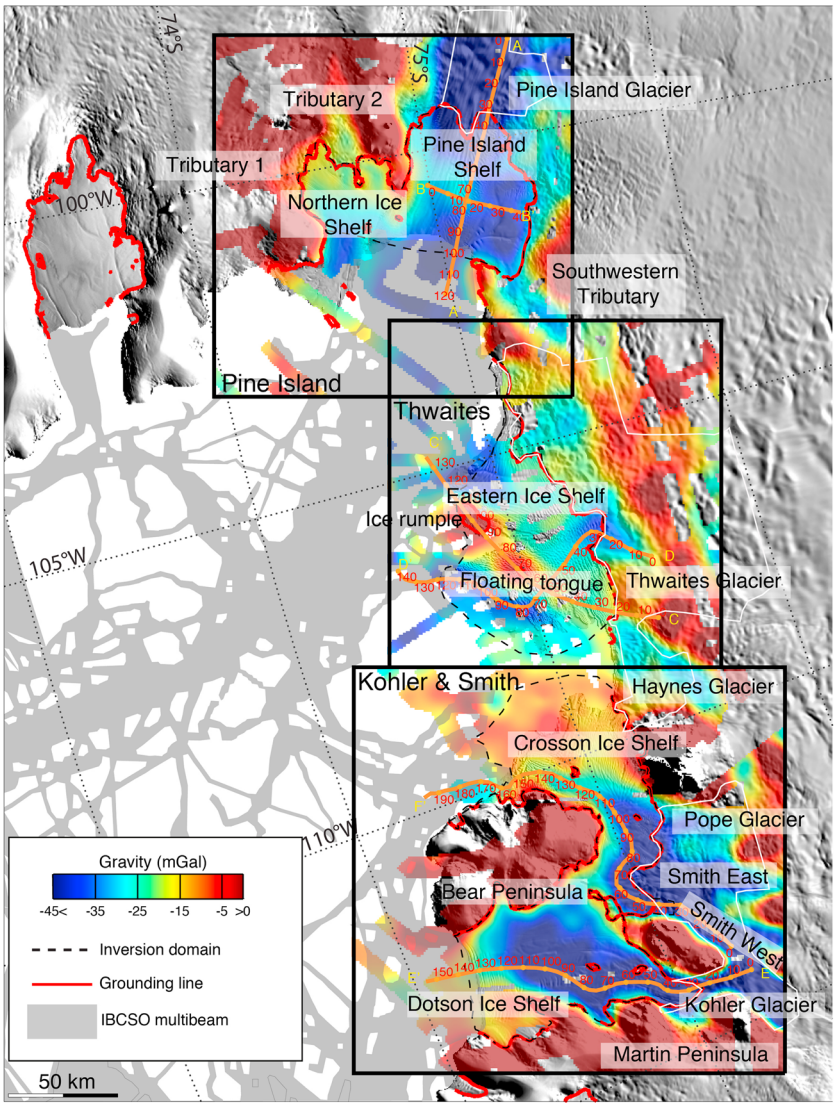

Figure 1. Free-air gravity anomalies in the Amundsen Sea Embayment (ASE) sector of West Antarctica with the Pine Island, Thwaites, Haynes, Pope, Smith, and Kohler glaciers overlaid on a MODIS mosaic of Antarctica from year 2004 on a gray scale. Areas mapped with multibeam echo sounding (MBES) are light blue. Glacier grounding lines from year 1996 are red. The limits of the gravity inversions are thin black dash lines within each black box. The limits of the MC inversion are thin white lines.

elevation and ice shelf thickness are from BEDMAP-2. Ice shelf thickness does not impact the gravity inversion since the ice shelves are in hydrostatic equilibrium, but it is used to calculate the height of the water column beneath ice shelves.

To complete the gravity observations and obtain gravity values at every point of our polar stereographic grid (71°S secant plane, 1000 m spacing), we employ a 3-D forward model of the gravity field based on an initial guess of the bed elevation, ice/water depth, and densities over the entire domain. We apply a 70 s full wavelength filter on the forward model gravity data. The initial bed combines the MC solution inland and IBCSO offshore (Figure S2). We merge the modeled and observed gravity by matching their mean value over land within a subregion of the MC domain. We allow for a 10 km wide transition boundary between the observed and modeled gravity. The approach of filling data gaps with modeled gravity minimizes edge effects along data gaps on the 3-D inversion [*Gourlet et al.*, 2016] and improves the 3-D inversion near large gravity anomalies such as mountain blocks.

For Pine Island, we employ an additional procedure with the AUV and seismic data. The initial bed solution combines MC on land, IBCSO on the ocean, and the AUV and seismic data beneath the shelf interpolated linearly with a Delaunay triangulation. We run the forward model to calculate the corresponding gravity field, form the difference between the forward model and the observed gravity, and best fit the result with a minimum curvature surface (Figure S3). The result is a gravity correction that we subtract from the OIB gravity field over the inversion domain. The corrected gravity is then completed with a forward model of the gravity, as described earlier, to fill data gaps with the rectangular domains of the inversion. In the case of Pine Island, the merging of observed and modeled gravity uses the mean gravity anomaly values in front of the glacier where MBES/IBCSO data are available.

The inversion domain extends from the MC domain to the MBES/IBCSO data or the limits of the gravity survey. We allow a 10 km wide smooth transition at the ocean boundary and at the grounding line. In the transition region, the inversion is modulated by a factor linearly varying between 0 (no gravity inversion) to 1 (full gravity inversion). No data inversion is performed on land (inversion factor is 0). We only invert the gravity data on the ice shelf and portions of the ocean not surveyed by MBES (inversion factor of 1). During the inversion, the unknown bed elevation is modified iteratively until we obtain the best match between modeled and observed gravity. The iteration stops when the standard deviation of the error gets lower than a user-provided value, here 0.1 mGal (1 milligal or 1 mGal = 10^{-5} m^2/s) (Figure S4). In order to provide a consistent topographic data set, we gridded our final bed elevation to the spacing of the MC data, here 450 m, which is not representative of the resolution of our gravity data (4.9 km).

To define an optimal average bed density beneath the glacier and the ocean, we calculate the rate of convergence of the solution in the gravity data misfit, i.e., modeled minus observed gravity, for densities varying from 2.2 to 3.4 g/cm^3 with a step of 0.05 g/cm^3. We find a minimum at a density of 2.88 g/cm^3 for Pine Island (Figure S5). We do not find a minimum for Thwaites and Smith/Kohler, so we use 2.88 g/cm^3 by default. A density greater than the standard 2.67 g/cm^3 is consistent with *Damiani et al.* [2014] for Thwaites (2.80 g/cm^3) and the presence of a rather pure crystalline bedrock in front of Pine Island shelf [*Lowe and Anderson*, 2003] but is not consistent with the presence of thick sediments in M2016. To determine the robustness of our solution to the density selection, we compare the results obtained on Thwaites Glacier using a lower density of 2.78 g/cm^3. We find a shift in bed elevation of 35 $\pm$ 13 m.

We use the gravity misfit, or modeled gravity minus observed gravity, to quantify the uncertainty of the inversion (Figure S4). To translate the gravity misfit into an error in bed elevation, we calculate the gravity field using GM-SYS 3-D obtained after shifting the bed solution by +100 m and comparing the results with the original gravity field. We find an average shift of 5.8 $\pm$ 0.5 mGal in gravity per 100 m of water for the inversion of the Kohler/Smith bathymetry. The statistics of the misfit (median and standard deviation) are 0.2 $\pm$ 3.7 mGal for Pine Island, 0.1 $\pm$ 3.7 mGal for Thwaites, and 0.01 $\pm$ 3.1 mGal for Kohler/Smith (Figure S4). These misfits translate into an uncertainty in bed elevation of 50 to 65 m. These numbers are a factor 2 to 3 lower than the $\pm$150 m errors quoted by *Studinger et al.* [2010] for a 2-D, unconstrained inversion, i.e., without AUV, seismic, MBES/IBCSO, and MC data.

3. Results

The bed elevation deduced from the gravity inversion closely follows variations in free-air gravity anomaly, as expected (Figure 2). The results indicate that the glaciers flow down deep troughs that extend on the seafloor beneath the ice shelves and onto the continental shelf (Figure S6) [*Jacobs et al.*, 2012]. Bed elevation beneath the ice shelves exceeds 800 m on Pine Island and Thwaites, 1200 m on Crosson, and 1500 m on Dotson.

Below the Pine Island Shelf, the difference in bed elevation between the AUV data and our inversion drops from -115 ± 101 m without gravity correction to -30 ± 25 m with correction, i.e., a reduction in standard deviation by four (Figure S7). For comparison, the difference between AUV and IBCSO is -22 ± 53 m. Along profile B-B', the difference between AUV and our solution is -16 ± 31 m versus -162 ± 101 for IBCSO (Figure S8). We are in good agreement with the grid from M2016 (Figure S9). The difference between their solution and ours improves from -35 ± 127 m without correction to -40 ± 103 m with correction (Figure S10). With respect to the seismic data, our solution improves from -38 ± 97 m to -37 ± 57 m with the correction (Figure S10), i.e., a factor 2. For comparison, the difference between M2016 and seismic is 21 ± 77 m (Figure S11). The improved AUV/seismic fitting from our solution also partially reflects the coarser resolution (2.5 km) of M2016.

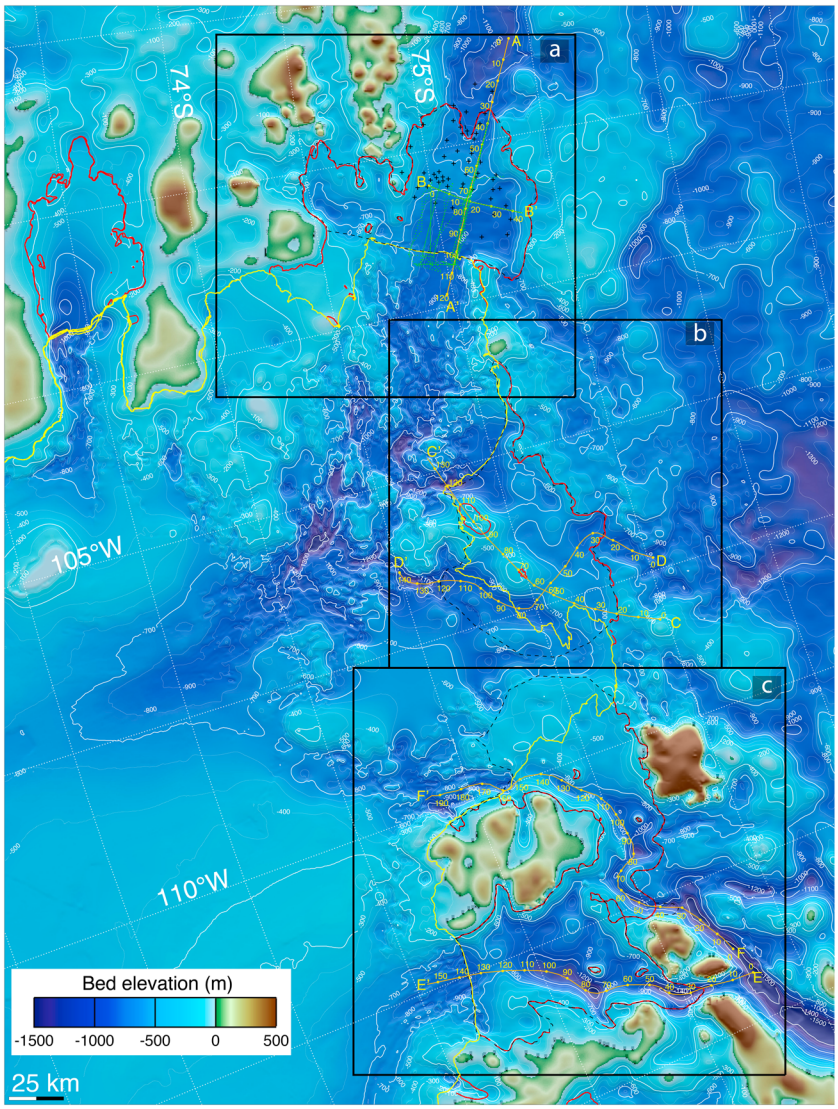

Figure 2. New bathymetry of the Amundsen Sea Embayment (ASE) of West Antarctica with the (a) Pine Island, (b) Thwaites/Haynes, and (c) Smith/Kohler glaciers. Grounding line positions are red (year 1996), ice front positions (year 2008) are yellow, AUV tracks are green, and seismic data are black crosses. Bed elevation is color coded from brown/yellow and green (above sea level) to light blue and dark blue (−1400 m), with light contours every 100 m and thick contours every 400 m. Profiles A-A′ to F-F′ in orange with dots every 10 km are shown in Figure 3.

Our solution confirms that the main channel beneath Pine Island Shelf is undercut by a north-south ridge with a bed elevation at 650 m depth, dropping by 50 m, 5 km south of km 60 in A-A′. Our solution offers a smooth transition with the MC topography and a seamless transition with MBES/IBCSO at the ice front. At the center of the 1996 grounding line, our bed elevation is 200 m lower than BEDMAP-2 and M2016 (red blotch in Figure S9 at 100°W, 75.25°S). This is an important feature controlling the glacier dynamics. The inversion also reveals a new channel beneath the northern ice shelf of Pine Island, not included in M2016, IBCSO, or BEDMAP-2. The northern channel is 600–800 m deep, with a water column of about 400 m (Figure S12). It connects with two northern tributaries of Pine Island Glacier (Figures 1 and S6). The inversion also highlights a second channel to the southwest, present in M2016 but not in IBCSO or BEDMAP-2, which connects with a southwestern tributary of Pine Island Glacier (Figures 1 and S6). This trough is deeper (about 700–800 m) than the northern channel and extends far inland with depths in the range of 800–1000 m (Figure 2).

For Thwaites, our inversion improves the transition with grounded ice and MBES/IBCSO compared to the inversion of *Tinto and Bell* [2011] along the eastern ice shelf and at the grounding line of the fastest-moving portion of the glacier (km 40–20 in profile D-D′, Figure 2). The bed elevation beneath the eastern ice shelf is on average

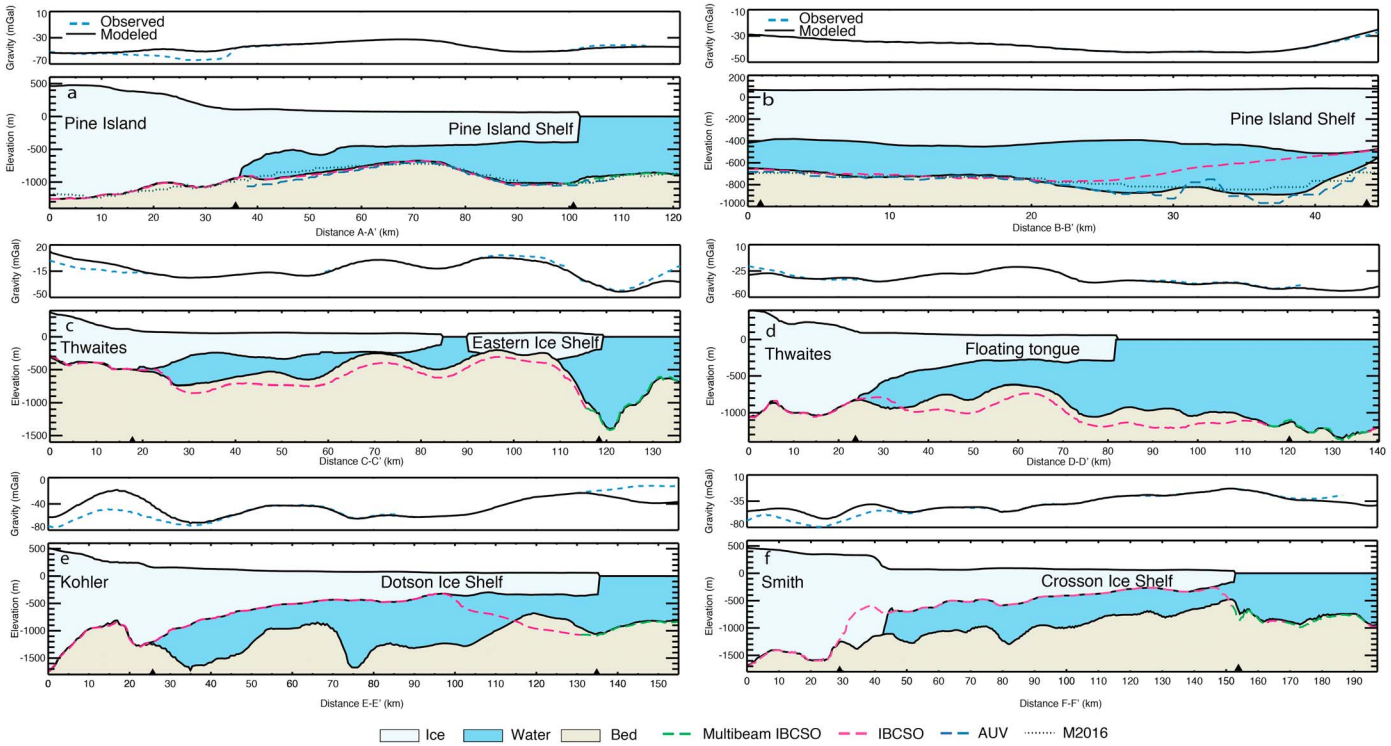

Figure 3. Surface and bed profiles along A-A′ to F-F′ (Figure 2) of (a and b) Pine Island, (c and d) Thwaites, and (e and f) Smith/Kohler glaciers associated with Crosson and Dotson ice shelves with the observed (blue dashed line) versus modeled (black continuous) gravity on the upper plot, surface elevation from BEDMAP-2, ice bottom elevation from BEDMAP-2, and bed elevation from this study (black), M2016 (black dotted line), multibeam echo sounding (MBES) from IBCSO (dashed green), IBSCO (dashed red), and Autosub Vehicle (AUV dashed blue). Ocean is blue, ice is light blue, and the glacier bed is light brown.

100 m higher than the results from *Tinto and Bell* [2011]. The water column thickness remains greater than 400 m, and bed elevation is about 700 m on average. The east-west ridge, which forms the ice rumples in front of the glacier, is broader and shallower in our solution but more consistent with our delineation of the grounding line from radar interferometry (km 70 and km 90–110 on C-C′, Figure 3). These improvements result from a 3-D inversion constrained with MC, MBES/IBCSO, and OIB gravity data collected after 2009.

Several channels undercut the east-west ridge of Thwaites, one from the east at 1000 m depth (km 70 in D-D′), rising to 700 m beneath the eastern ice shelf (Figure 2). A second one is found along the central part (km 60 in D-D′), starting at 1000 m depth, but shallowing to 600–650 m as it intersects the east-west ridge (km 50–60 in C-C′). A third pathway is found at km 25–30 along C-C′ at a depth of 700 m. At the grounding line, we find a 100 m sill in topography at km 25 on D-D′ between the 1996 and 2011 grounding lines along the main trough of Thwaites.

The most significant improvements in sub–ice shelf mapping are for the Crosson and Dotson ice shelves since these cavities had virtually been unexplored (Figure 2). The inversion reveals deep channels beneath both ice shelves. The bed trough beneath Crosson is at 800 m depth on average and deepening to 1200 m inland where the glacier has undergone a fast retreat. The trough connects with Pope, Smith East, and Smith West. The grounding line of these glaciers follows an east-west ridge with several mounds at 600 m depth. The main bed trough rises to 500 m at km 150 along F-F′, near the ice shelf front. The shallow part of the trough at km 150 is only 7–8 km wide. A set of three OIB gravity lines constrains that ridge, which lays only 1 km south of the MBES/IBCSO data, hence relatively well constrained by observations (Figures 1 and S4). If a narrow passage exists, it has to be narrower than the resolution of the gravity data, or 5 km.

The channel beneath Dotson is deeper, exceeding 1500 m below sea level at km 30 and 75 in E-E′ (Figure 2). At km 30, the overdeepened bed coincides with the confluence of Kohler, a tributary glacier to the west, and a narrowing of the ice shelf to fit the 8 km wide terminal valley of Kohler. The bed rises rapidly along that terminal valley. Near the ice front, at km 125 on E-E′, we find the shallowest part of the trough, an east-west ridge at 750 m depth that connects Bear Peninsula and Martin Peninsula. The ridge is about 25 km wide.

The water column is more than 400 m thick. The inversion is constrained by MBES/IBCSO along the ice shelf front. We also note an 8 km channel connecting Crosson and Dotson, 700 m in depth, with a water column of 200 m, hence deep enough for water exchanges between the two cavities. Note that all the ice rises have been preserved in the inversion. The presence of many of them on the ice shelves could give the impression that Dotson Ice Shelf—and to some extent Crosson Ice Shelf—has a shallow cavity, but our results reveal that these ice rises correspond to isolated peaks rather than major ridges. The deep ice shelf cavities beneath Crosson and Dotson do not exist in IBCSO and BEDMAP-2 (Figure S12).

4. Discussion

The results obtained beneath Pine Island Shelf confirm and complete M2016 by providing a better fit with the MC reconstruction inland and the MBES/IBCSO offshore. The seamless map resolves the pinning point at the center of the glacier (5 km to the east of A-A′ at km 45 in Figure 2), which plays an important role in the ice dynamics [*Joughin et al.*, 2016]. This pinning point cannot be resolved from gravity alone because of data resolution (about 5 km) but is reproduced on land with MC. The new map reveals a channel to the north that connects with shallow tributaries of Pine Island and a deeper channel to the southwest which connects with a deep tributary.

In this region, the warmest waters have been consistently observed below 700 m, and most of the decadal to subdecadal variability in ocean temperature is confined to shallower depths [*Dutrieux et al.*, 2014]. Hence, the propencity of the region to harbor trough sills that would block access to the ice front for the warmest waters is significant. The east-west ridge in Pine Island between 650 and 700 m depth plays a major role in controlling the advection of CDW to the sub–ice shelf cavity [*Dutrieux et al.*, 2014]. The deepest part of the ridge, a saddle in the southwest, is about 750 m, such that the inner part of the cavity leading to the deep (>1000 m) grounding line of the fast-flowing trunk is only accessed by the shallower, more variable ocean heat content. Similarly, access to a deep southern tributary in the outer part of the cavity may be limited to a water shallower than 750 m. The northern Pine Island channel is slightly shallower, but the ice shelf draft there (<450 m) is already self-limiting.

Beneath the Thwaites eastern ice shelf and the central ice tongue, the bed elevation also narrows down to about 700 m depth. These CDW pathways are, therefore, deep enough to enable intrusion of CDW but limited to shallower, more variable waters above the more consistently warm CDW.

Based on our results, considerable thinning (>100 m) would be required to detach the Thwaites eastern ice shelf from its pinning points (Figure 3), which makes this ice shelf more stable than could be deduced from the surface appearance of the ice rumples. At the center of Thwaites, near the grounding line, we find a shallower sill in topography at km 30 in D-D′, which is consistent with the rate of fast, continuous, and sustained retreat of the glacier at that location [*Rignot et al.*, 2014].

Beneath the Crosson, we find a deep trough that could channelize CDW deep into the cavity but is undercut by a narrow ridge at km 150 in F-F′. The ridge is a robust feature of the inversion, but the gravity data are limited to a spatial resolution of 4.9 km. To determine if the ridge blocks the access of CDW or if a passage narrower than 4.9 km exists, higher-resolution data and/or complementary observations would be required.

Beneath the Dotson, we find a similar but broader (20 km for Dotson versus less than 10 km for Crosson) channel with a shallow passage near the ice front, however, deep enough (700–750 m) to enable CDW intrusion. Ice shelf melt rates inferred from remote sensing data collected in 2003–2009 are lower on Dotson (7.8 m/yr) than Crosson (11.9 m/yr) [*Rignot et al.*, 2013]. The bathymetry suggests that CDW has an easier access beneath Dotson Ice Shelf than beneath Crosson Ice Shelf, which is opposite to the contrast in ice shelf melt rate. We conclude that the difference in ice shelf melt rate does not reflect differences in sub–ice shelf bathymetry but must reflect differences in the source of CDW. Indeed, a lighter, cooler version of modified CDW accesses Dotson Ice Shelf through the Dotson/Getz western trough on the continental shelf [*Jacobs et al.*, 2013] versus the Pine Island eastern trough on the continental shelf that accesses the Crosson Ice Shelf.

Immediately inland of our inversion, the misfit between modeled and observed gravity is significant (Figure S2), up to 16 mGal, which suggests that our density selection is not optimum. A more complete inversion would require a more complex geology and the presence of sediments. The misfit, however, decreases inland and does not affect our solution on land where we use the MC reconstruction. To improve the results

beneath the cavities of Thwaites, Crosson, and Dotson ice shelves, additional constraints such as AUV or seismic would be needed. In the case of Pine Island Glacier, the addition of such data reduced errors from 100 m to 25 m. Without additional constraints, errors in bed elevation probably remain above 64 m. The addition of new data would not change the location of the main troughs, but it would also refine spatial details and, in particular, address the possibility of narrow, unresolved channels (<5 km).

The novel bathymetry reveals the natural pathways for CDW to access the glaciers, which are critical for ocean modeling and ice sheet flow modeling. The inversion is affected by uncertainties in bed elevation, especially in unconstrained areas. The mapping of sub–ice shelf channels from gravity, however, provides invaluable guidelines for future hydrographic and bathymetric surveys. A seamless topography between MC and IBCSO also remains a long awaited critical product in this part of West Antarctica for ice-sheet/ocean numerical modeling studies. Prior mappings, such as BEDMAP-2, do not provide reliable geometries beneath the shelves or realistic transitions at the grounding lines. The new bathymetry should help reduce uncertainties in numerical model simulations. A similar methodology combining MC, IBCSO, OIB gravity, and other data should be applied to many other ice shelves around Antarctica that remain unexplored.

5. Conclusions

We presented a novel 3-D inversion of the OIB gravity data in the ASE sector of West Antarctica constrained at the land boundary by a high-resolution reconstruction of bed topography from mass conservation, offshore by MBES/IBCSO data, and in between by AUV and seismic data in the case of Pine Island. The results refined the details of the Pine Island sub–ice shelf cavity, suggest a slightly shallower cavity beneath Thwaites and a smoother transition to the grounded ice, and reveal deep channels beneath the Crosson and Dotson Ice Shelves that were not known previously. These troughs provide natural access of CDW to the cavities up to a range of about 700 m depth over the entire glacier system. We expect these data to be of considerable importance for interpreting recent and past changes of this sector of West Antarctica, assist numerical models of ocean circulation, ice sheet flow, and ice-ocean interactions. The data will provide guidelines for future and detailed in situ surveys.

Acknowledgments
This work was funded by grants from the National Aeronautics and Space Administration's Cryosphere Science Program, Operation IceBridge Mission, and Interdisciplinary Science program at the University of California Irvine and at Caltech's Jet Propulsion Laboratory. We thank the NASA-funded OIB instrument team for their achievements in collecting OIB data pole-to-pole since 2009 and making this kind of study possible. We also thank A. Muto and K. Tinto for useful discussions at the project inception and P. Dutrieux, L. Peters, A. Muto, and S. Anandakrishnan for sharing the AUV and seismic data. The bed topography described herein is available from the authors and will be posted at NSIDC.

References

Arndt, J. E., et al. (2013), The International Bathymetric Chart of the Southern Ocean (IBCSO) Version 1.0—A new bathymetric compilation covering circum-Antarctic waters, *Geophys. Res. Lett.*, *40*, 3111–3117, doi:10.1002/grl.50413.

Cochran, J. R., and R. E. Bell (2010), *IceBridge Sander AIRGrav L1B Geolocated Free Air Gravity Anomalies*, NASA Distributed Active Archive Center at the National Snow and Ice Data Center, Boulder, Colo. [Available at http://nsidc.org/data/iggrv1b.html. Digital media, updated 2014.]

Damiani, T. M., T. A. Jordan, F. Ferraccioli, D. A. Young, and D. D. Blankenship (2014), Variable crustal thickness beneath Thwaites Glacier revealed from airborne gravimetry, possible implications for geothermal heat flux in West Antarctica, *Earth Planet. Sci. Lett.*, *407*, 109–122.

Dutrieux, P., J. De Rydt, A. Jenkins, P. R. Holland, H. Kyung Ha, S. Hoon Lee, E. J. Steig, Q. Ding, E. Povl Abrahamsen, and M. Schroder (2014), Strong sensitivity of pine island ice-shelf melting to climatic variability, *Science*, *343*, 174–178.

Favier, L., G. Durand, S. L. Cornford, G. H. Gudmundsson, O. Gagliardini, F. Gillet-Chaulet, T. Zwinger, A. J. Payne, and A. M. Le Brocq (2014), Retreat of Pine Island Glacier controlled by marine ice-sheet instability, *Nat. Clim. Change*, *4*, 117–121.

Fretwell, P., et al. (2013), Bedmap2: Improved ice bed, surface and thickness datasets for Antarctica, *Cryosphere*, *7*, 375–393.

Gourlet, P., E. Rignot, A. Rivera, and G. Casassa (2016), Ice thickness of the northern half of the Patagonia Icefields of South America from high-resolution airborne gravity surveys, *Geophys. Res. Lett.*, *43*, 241–249, doi:10.1002/2015GL066728.

Holt, J. W., D. D. Blankenship, D. L. Morse, D. A. Young, M. E. Peters, S. D. Kempf, T. G. Richter, D. G. Vaughan, and H. F. J. Corr (2006), New boundary conditions for the West Antarctic Ice Sheet: Subglacial topography of the Thwaites and Smith glacier catchments, *Geophys. Res. Lett.*, *33*, L09502, doi:10.1029/2005GL025561.

Hughes, T. (1981), The weak underbelly of the West Antarctic Ice Sheet, *J. Glaciol.*, *27*, 518–525.

Jacobs, S. S., A. Jenkins, C. F. Giulivi, and P. Dutrieux (2011), Stronger ocean circulation and increased melting under Pine Island Glacier ice shelf, *Nat. Geosci.*, *4*(8), 519–523.

Jacobs, S. S., A. Jenkins, H. Hellmer, C. Giulivi, F. Nitsche, B. Huber, and R. Guerrero (2012), The Amundsen Sea and the Antarctic ice sheet, *Oceanography*, *25*(3), 154–163.

Jacobs, S., C. Giulivi, P. Dutrieux, E. Rignot, F. Nitsche, and J. Mouginot (2013), Getz Ice Shelf melting response to changes in ocean forcing, *J. Geophys. Res. Oceans*, *118*, 4152–4168, doi:10.1002/jgrc.20298.

Jenkins, A., P. Dutrieux, S. S. Jacobs, S. D. McPhail, J. R. Perrett, A. T. Webb, and D. White (2010), Observations beneath Pine Island Glacier in West Antarctica and implications for its retreat, *Nat. Geosci.*, *3*, 468–472.

Joughin, I., B. E. Smith, and B. Medley (2014), Marine ice sheet collapse potentially under way for the Thwaites Glacier Basin, West Antarctica, *Science*, *344*, 735–738.

Joughin, I., D. E. Shean, , B. E. Smith, and P. Dutrieux (2016), Grounding line variability and subglacial lake drainage on Pine Island Glacier Antarctica, *Geophys. Res. Lett.*, *43*, 9093–9102, doi:10.1002/2016GL070259.

Lowe, A. L., and J. B. Anderson (2003), Evidence for abundant subglacial meltwater beneath the paleo-ice sheet in Pine Island Bay, Antarctica, *J. Glaciol.*, *49*, 125–138.

Leuschen, C., P. Gogineni, F. Rodriguez-Morales, J. Paden, and C. Allen (2010), *IceBridge MCoRDS L2 Ice Thickness*, Natl. Snow and Ice Data Cent., Boulder, Colo., Digital media, updated 2015.

Morlighem, M., E. Rignot, H. Seroussi, E. Larour, H. Ben Dhia, and D. Aubry (2011), A mass conservation approach for mapping glacier ice thickness, *Geophys. Res. Lett.*, *38*, L19503, doi:10.1029/2011GL048659.

Muto, A., L. E. Peters, K. Gohl, I. Sasgen, R. B. Alley, S. Anandakrishnana, and K. L. Rivermana (2016), Subglacial bathymetry and sediment distribution beneath Pine Island Glacier ice shelf modeled using aerogravity and in situ geophysical data: New results, *Earth Planet. Sci. Lett.*, *433*, 63–75.

Nitsche, F. O., S. S. Jacobs, R. D. Larter, and K. Gohl (2007), Bathymetry of the Amundsen Sea continental shelf: Implications for geology, oceanography, and glaciology, *Geochem. Geophys. Geosyst.*, *8*, Q10009, doi:10.1029/2007GC001694.

Parizek, B. R., K. Christianson, S. Anandakrishnan, R. B. Alley, R. T. Walker, R. A. Edwards, D. S. Wolfe, G. T. Bertini, S. K. Rinehart, R. A. Bindschadler, and S. M. J. Nowicki (2013), Dynamic (in)stability of Thwaites Glacier, West Antarctica, *J. Geophys. Res. Earth Surf.*, *118*, 638–655, doi:10.1002/jgrf.20044.

Parker, R. L. (1973), The rapid calculation of potential anomalies, *Geophys. J. Int.*, *31*, 447–455.

Rignot, E. (2008), Changes in West Antarctic ice stream dynamics observed with ALOS PALSAR data, *Geophys. Res. Lett.*, *35*, L12505, doi:10.1029/2008GL033365.

Rignot, E., S. Jacobs, J. Mouginot, and B. Scheuchl (2013), Ice-shelf melting around Antarctica, *Science*, *341*, 266–270.

Rignot, E., J. Mouginot, M. Morlighem, H. Seroussi, and B. Scheuchl (2014), Widespread, rapid grounding line retreat of Pine Island, Thwaites, Smith, and Kohler glaciers, West Antarctica, from 1992 to 2011, *Geophys. Res. Lett.*, *41*, 3502–3509.

Studinger, M., C. T. Allen, W. Blake, L. Shi, S. H. Elieff, W. B. Krabill, J. G. Sonntag, S. Martin, P. Dutrieux, A. Jenkins, and R. E. Bell (2010), Mapping Pine Island Glacier's sub-ice cavity with airborne gravimetry, Abstract C11A-0528 presented at 2010 Fall Meeting, AGU, San Francisco, Calif., 13–17 Dec.

Thomas, R., et al. (2004), Accelerated sea level rise from West Antarctica, *Science*, *306*, 255–258.

Tinto, K. J., and R. E. Bell (2011), Progressive unpinning of Thwaites Glacier from newly identified offshore ridge: Constraints from aerogravity, *Geophys. Res. Lett.*, *38*, L20503.

Vaughan, D. G., H. F. J. Corr, F. Ferraccioli, N. Frearson, A. O'Hare, D. Mach, J. W. Holt, D. D. Blankenship, D. L. Morse, and D. A. Young (2006), New boundary conditions for the West Antarctic ice sheet: Subglacial topography beneath Pine Island Glacier, *Geophys. Res. Lett.*, *33*, L09501, doi:10.1029/2005GL025588.